Evaluation and Field Testing of the Dan Ryan Rapid Transit Structure

ANDREW E. N. OSBORN and MICHAEL J. KOOB

ABSTRACT

The Dan Ryan rapid transit structure is a 40-span, 4,000-ft-long elevated structure that carries Chicago Transit Authority (CTA) rapid transit trains into and out of the Chicago Loop. The structure, which was completed in 1969, consists of welded stringers and is supported by steel box-girder bents. Splices in the stringers are field bolted. The steel stringers carry two sets of track on a ballasted concrete deck. In January 1978 major brittle fractures occurred in three of the steel box-girder bents. Since discovering the bent fractures, CTA inspectors found two long cracks in the bottom of the stringers. These cracks were found to originate at welded lateral gusset-plate connections. Approximately 1,800 lateral gussets are used in the 40-span system to attach lateral bracing. Each gusset plate contains a cutout to accommodate the vertical stiffener of the stringer. This detail creates a short gap between the cutout of the gusset and the vertical stiffener. An extensive investigative study of seven spans of the superstructure was carried out to assess the fatigue sensitivity of the stringers with the lateral gusset-plate connections. The study included a review of details used in the structure, field instrumentation and testing, an analytical review, in-depth examination of gusset-plate connections, examination and testing of samples that contain cracks, and the development of retrofits. The information collected during the study, particularly the field testing data, is reviewed. Reviews are also made of the fractographic examination conducted on a sample that contains a 4-in. crack and the in-depth inspection findings. As part of this study retrofits were developed to either shield the crack origin from stress or to increase the gap between the gusset-plate cutout and the vertical stiffener.

A post-construction investigation of the Dan Ryan elevated rapid transit structure between 17th and 23rd streets in Chicago was conducted for the Chicago Transit Authority (CTA). The purpose of the investigation was to evaluate the sensitivity of welded details in the structure to fatigue.

Field work consisted of in-depth inspection and strain-gauge instrumentation of critical conditions in the structure. This work was carried out between August and November 1982. Office activities included identification of critical details, structural analyses, evaluation of test data, and development of recommendations for retrofitting and ongoing inspection.

DESCRIPTION OF STRUCTURE

The CTA's Lake-Dan Ryan rapid transit line provides direct service between the south and west sectors of Chicago. The structure under investigation consists of 40 spans, with a total length of about 4,000 ft. A plan view of the structure is shown in Figure 1.

The viaduct structure is of welded steel construction and was completed in June 1969. The superstructure consists of continuous and suspended plate girders (stringers) with a cast-in-place, U-shaped concrete deck. Figure 2 shows a typical structural cross section at a hammer-head pier. In addition to single-column supports referred to as pier, the structure includes seven inverted U-shaped supporting structures that have double columns; these are referred to as bents. Three of these bents sustained major fractures in January 1978 (1). Six stringers are used in each of spans 2-16 (double track); four stringers are used in each of spans 1 and 17-34 (double track); and spans 35NB-37NB and 35SB-40SB use two stringers (single track). Stringers are curved in spans with sharp curvature.

The plate girders are provided with vertical stiffeners spaced approximately 4 ft apart and horizontal gusset plates spaced at approximately 8 or 16 ft, depending on location. The gusset plates are located about 4 in. above the bottom flange of the stringers. Deep, channel-shaped diaphragms are bolted to stiffeners along the web of the channel and gusset plates at the channel flange. Lateral bracing members are also bolted to the gusset plates. Lateral bracing consists of angle K bracing to bent 34 and structural tee X bracing beyond bent 34. A plan view of three spans that shows the variation in framing systems is presented in Figure 3. The underside of span 15 is shown in Figure 4; it shows the lateral bracing system typical of spans 2-16.

Lateral gusset plates are welded to the webs of stringers, with the vertical stiffener fitting into a cutout in the gusset plate, as shown in Figures 5 and 6. In spans 1-27 the cutouts are close fitting, and fillet welds were used for the gusset plate to stringer web connection. In spans 28 and above there is an approximate 0.5-in. gap between the cutout edge and the stiffener, and the gusset plates were single-bevel groove welded to the web. Back-up bars were used to make the groove weld connections in spans 35-40. The back-up bars or gusset plates were attached with short intermittent fillet welds for fit-up before completing the groove welds. The termination of all these welds represents conditions that are sensitive to fatigue (2).

In 1978 the CTA found an 8-in.-long crack in span 35 that originated in the gap between the gusset-plate cutout and the vertical stiffener. Holes were drilled at both the top and bottom ends of the crack as a retrofit measure.

In fall 1982 a crack was found in the stringer of span 15. Again the crack originated at the gap between the vertical stiffener and the gusset-plate cutout. The crack had propagated down through the bottom flange and also up about 12 in. into the web. A hole was drilled at the top end of the crack and a cover plate was bolted to the bottom flange across the crack. An exterior view of the crack is shown in

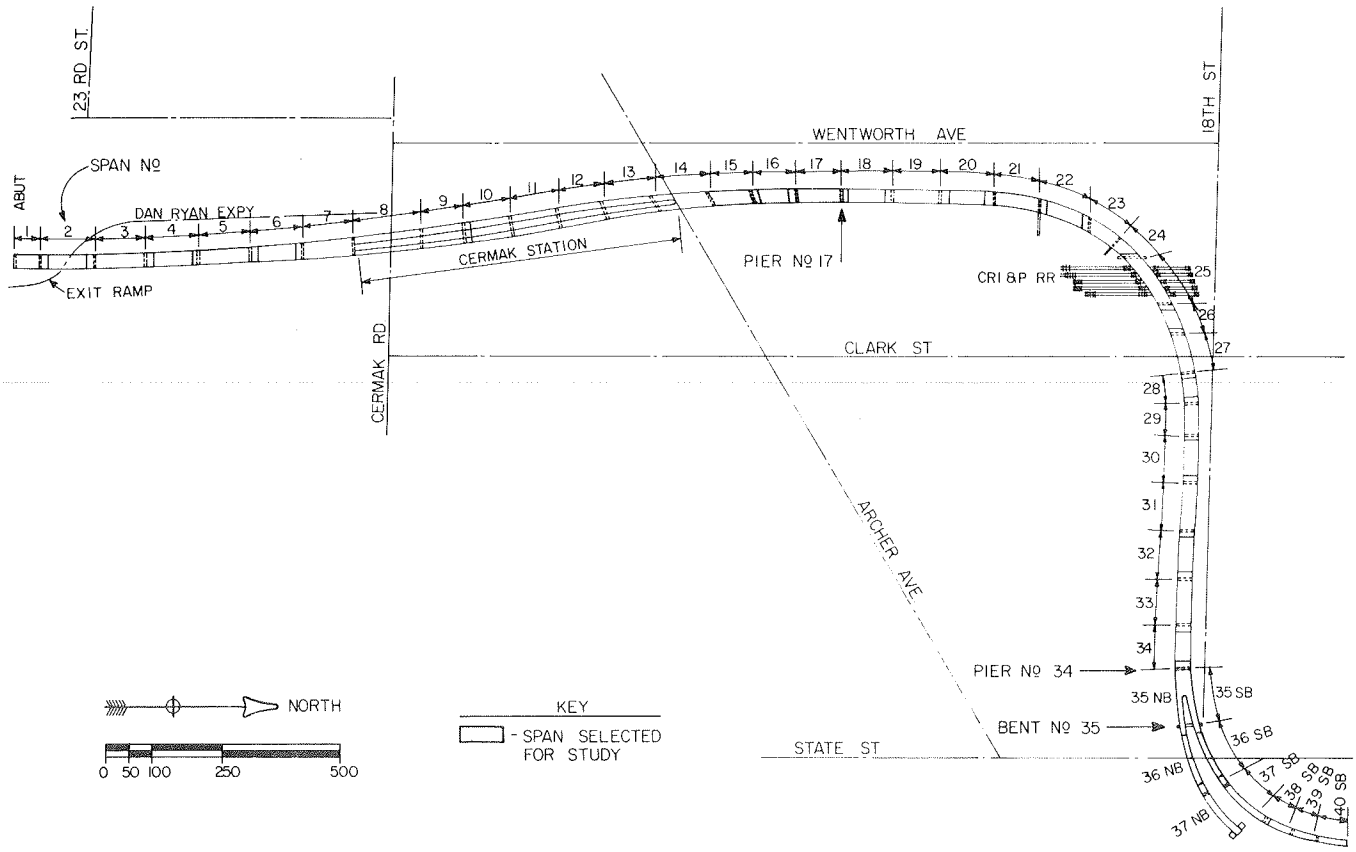

FIGURE 1 Plan of Dan Ryan elevated structure under study.

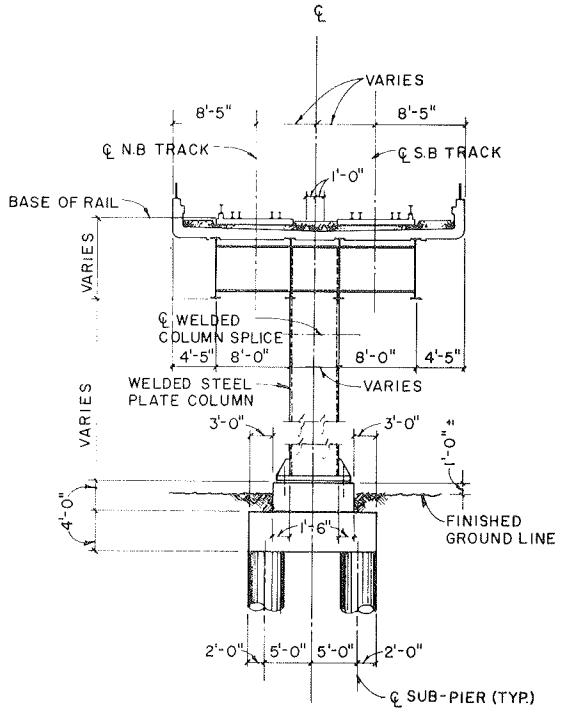

FIGURE 2 Cross section of structure at a hammer-head pier.

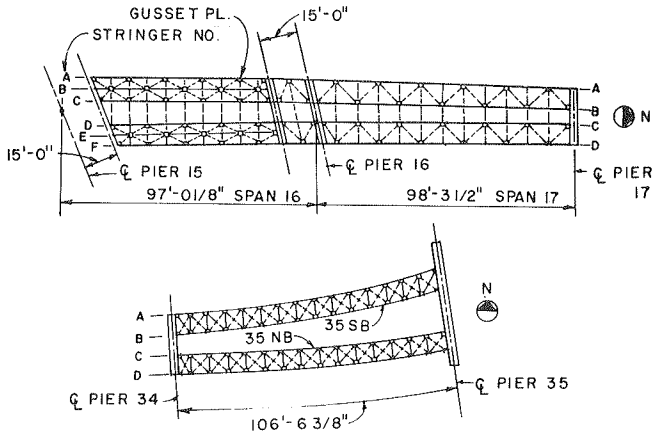

FIGURE 3 Schematic showing the three general types of framing.

Figure 7. Staining in Figure 7 is from the cutting oil used for drilling.

The discovery of these cracks increased concern over the fatigue sensitivity of the lateral gusset-plate connection and precipitated this evaluation study.

DESCRIPTION OF WORK

The study consisted of five tasks, as follows:

1. Conduct a limited structural analysis of the viaduct superstructure to determine theoretical stress ranges at fatigue-sensitive details,
2. Install strain-gauge instrumentation and per-

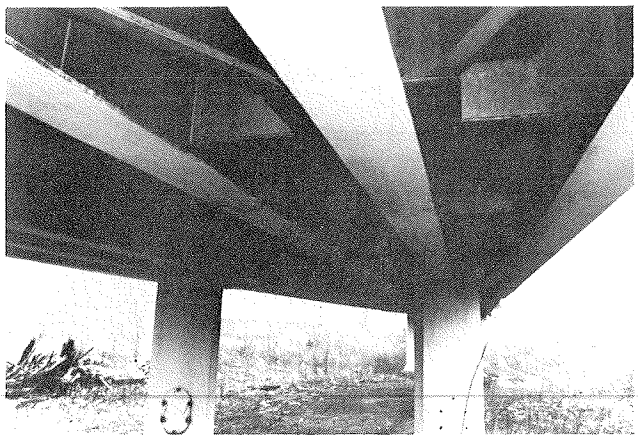

FIGURE 4 View of framing on the underside of span 15.

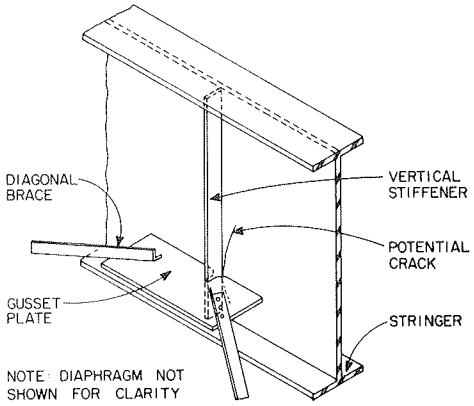

FIGURE 5 Gusset-plate connection: schematic view.

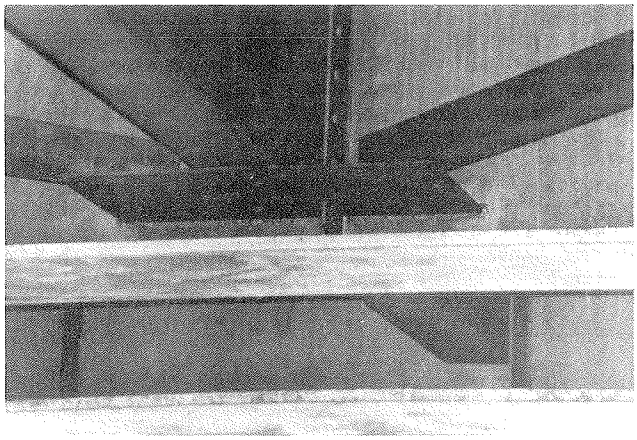

FIGURE 6 Gusset-plate connection: typical detail.

form tests at selected locations in several spans under normal and controlled loadings,

3. Perform a high-quality fatigue crack inspection of gusset-plate welds in the same spans where instrumentation was installed,

4. Remove steel samples for visual and microscopic evaluation, and

5. Develop a structural retrofit for the gusset-plate detail.

FIGURE 7 Appearance of retrofitted crack located in span 15.

Structural Analysis

A structural analysis was performed on a simplified analytical model of the elevated structure. The steel stringers were assumed to act compositely with the concrete deck, and curvature effects were included in the model. The stiffnesses of the box bents included consideration of soil-structure interaction. The lateral rigidity of the U-shaped deck was modeled; however, the torsional rigidity provided by lateral bracing and diaphragms was omitted.

Dead loads were based on information contained in the design drawings. Live load was based on the fatigue and deflection loading criteria of 19.5 kips per axle established by CTA (see Figure 8). These loads are higher than those used when the structure was designed because of the introduction of the heavier 2600 series cars in 1981. An impact factor of 40 percent was added; however, testing discussed later indicated that impact effects were much smaller. Thus the tabulated stresses reported here do not include impact.

The actual train weights were somewhat less than the design loading criteria. Empty train car weights vary from 45 to 54.3 kips for all series of cars used on this structure. The weight of passengers that can occupy the seat and aisle area is expected to be about 26 kips under maximum loading conditions. Normal rider weight during rush-hour traffic, however, is probably closer to 16 kips per car, or 4 kips per axle. Thus normal rush-hour axle loads are probably in the vicinity of 17.5 kips. This estimate has been used to compare theoretical and field-measured results. On a weekday 78 eight-car trains, 131 four-car trains, and 20 two-car trains traverse the line in both directions. On weekends the traffic is lighter. Altogether, about 1,400 trains pass in each direction every week.

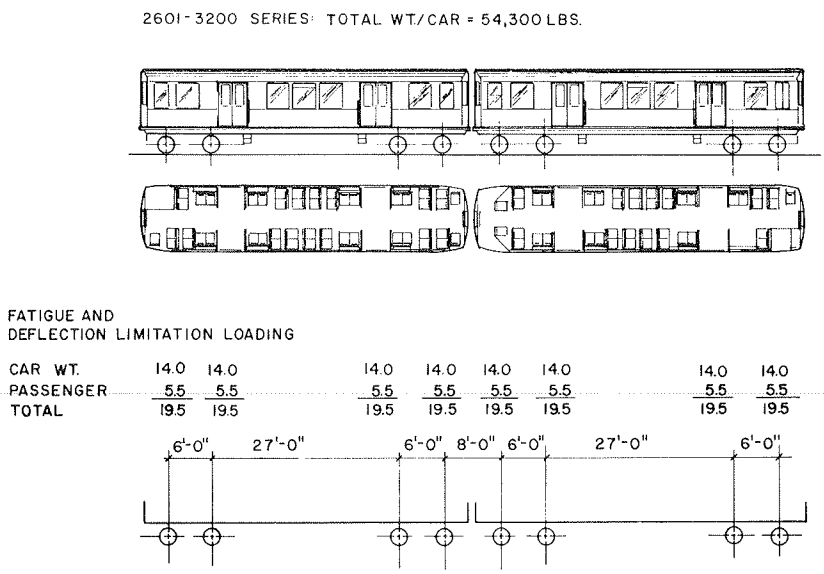

FIGURE 8 Elevation and axle load pertaining to transit car.

TABLE 1 Calculated Midspan Stringer Stresses at Level of Gusset Plate

Span No.	Approximate Dead-Load Stress (ksi)	Live-Load Stress Range (ksi)	
		Two-Car Train	Eight-Car Train
1	3.0	1.4	1.1
2	10.8	2.1	2.1
3	10.3	3.8	3.1
4	10.5	1.9	1.9
5	11.6	1.6	3.1
6	10.8	1.8	1.8
7	10.1	3.2	2.6
8	17.3	3.3	3.0
9	9.0	2.9	2.3
10	15.7	2.0	1.8
11	12.4	2.7	2.4
12	10.4	2.0	1.8
13	10.1	2.4	2.1
14	15.1	3.1	2.9
15	6.2	2.6	2.1
16	8.1	2.5	2.5
17	11.8	4.0	3.4
18	11.7	2.3	2.3
19	8.8	3.6	3.0
20	11.7	2.3	2.3
21	10.5	3.9	3.2
22	9.2	1.7	1.7
23	6.2	2.8	2.2
24	6.1	1.4	1.4
25	15.9	3.8	3.5
26	5.9	1.5	1.5
27	7.4	2.1	1.9
28	3.9	1.0	1.0
29	3.1	1.8	1.4
30	9.6	1.9	1.9
31	9.5	3.9	3.1
32	8.6	1.7	1.7
33	10.1	3.8	3.1
34	9.2	2.0	2.0
35NB	8.5	2.8	2.3
35SB	7.5	2.6	2.1
36NB	12.2	1.9	1.9
36SB	11.6	1.7	1.7
37NB	17.4	2.8	2.7
37SB	10.8	2.9	2.5
38SB	8.1	1.2	1.2
39SB	6.1	1.4	1.2
40SB	6.1	1.3	1.1

Note: Live-load tabulation based on axle load of 19.5 kips. In curved spans the longest storage span was analyzed.

In calculating the total dead-load stresses, noncomposite action was assumed for the weight of the steel stringers, steel bracing, and concrete deck. Composite action was assumed for the remaining dead loads and all live loads. This procedure increased the calculated dead-load stresses by about 30 percent when compared to an analysis based on a fully composite structure. The calculated stresses from the structural analysis are given in Table 1.

Instrumentation

Locations in seven spans and three supports were selected for strain-gauge instrumentation. Altogether, 85 gauges were installed. The instrumented areas included both simple and continuous spans, curved spans, and spans where relatively high levels of stress range were expected.

Strain gauges were installed primarily on webs of stringers adjacent to gusset plates, on stringer flanges, and on cross-bracing members. Figure 9 shows an installation adjacent to a gusset plate. Gauges were also installed on the webs and flanges of box bents and on a hinge link. Details of the strain-gauge layout are shown in Figure 10.

Installation Details

Locations in spans 15-17, 21, 22, 35, and 36, and in bents 17, 34, and 35 were instrumented. Single-element, 0.25-in. foil-type strain gauges were bonded to the steel structure by using long-life epoxy adhesive. Copper lead wires of 18 or 22 gauge were soldered to the strain gauges, and the gauges were waterproofed. The entire installation was intended to be durable so that readings could be taken for several years, if desired. The lead wires were extended to three primary junction areas located in bents 16, 21, and 35 and connected to multiple socket connectors. In this way the strain reading equipment could be moved from bent to bent instead of running all the lead wires to one location.

Data Acquisition

The strains were measured by using a Hewlett-Packard

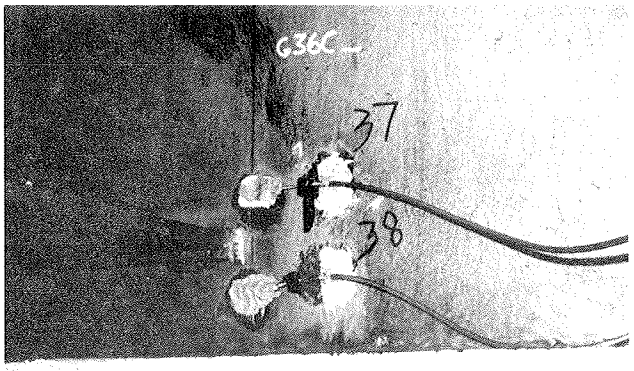

FIGURE 9 Type A gauge installation on web of stringer adjacent to gusset plate.

HP3054 Data Acquisition System coupled to an HP9826 computer. The data logger had the capability of measuring and transmitting approximately 50 channels of voltage data per second. Five gauges were monitored at one time, which permitted about 10 measurements per gauge per second to be recorded for each train. Gauges at comparable locations were generally read together to provide comparisons on the basis of a single train passage.

The accuracy of the data-logging equipment was verified by recording strain data using a strip-chart analog recorder and a peak read digital strain indicator. Both of these instruments gave strain values that were close to those recorded with the digital data-logging equipment. The analog recorder also indicated that there were no high-frequency stress cycles that were being missed because of the sampling rate of the data acquisition system.

Data were recorded dynamically during passages of commuter trains, and both statically and dynamically

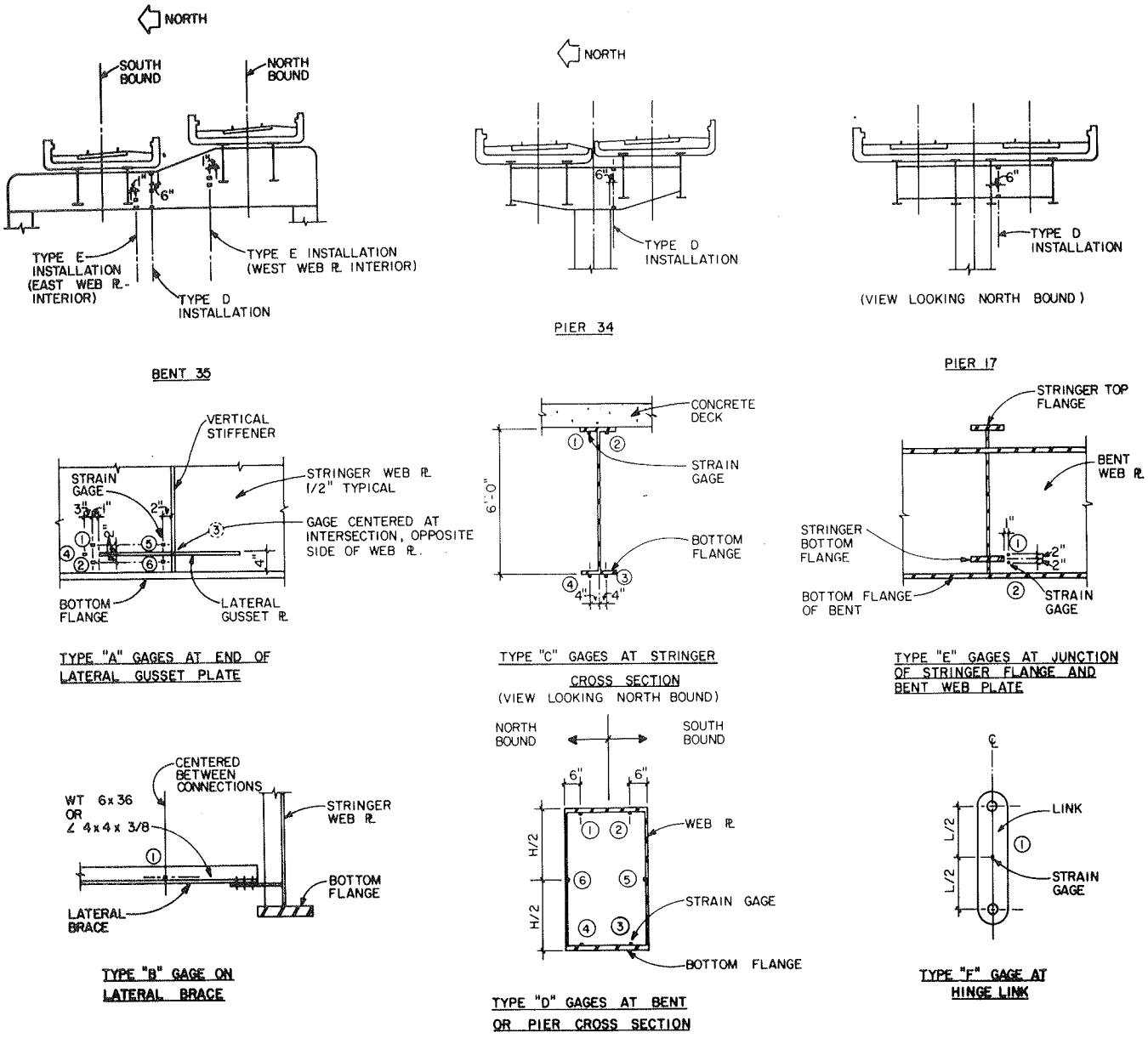

FIGURE 10 Location and designation of strain gauges.

TABLE 2 Comparison of Stress Ranges Measured on Selected Spans

Span No.	Test Train: Two-Car Train Dynamic (ksi)	Test Train: Two-Car Train Static (ksi)	Test Train: Two-Car Train Impact Dynamic[a] (ksi)	Commuter Trains: Four-Car Train Dynamic (ksi)	Commuter Trains: Eight-Car Train Dynamic (ksi)	Test Train: Eight-Car Train Dynamic (ksi)	Test Train: Eight-Car Train Static (ksi)
15SB	1.5	1.6	-	1.4	1.3	1.3	1.3
16SB	1.5	1.4	-	1.6	1.4	1.5	1.5
17NB	1.9	2.0	-	2.0	1.9	1.7	1.8
21SB	2.0[b]	2.0[b]	-	2.0[b]	1.8[b]	1.9[b]	1.9[b]
22SB	1.6	1.5	-	1.7	1.6	1.7	1.6
35NB	2.1	2.0	1.9	1.9	1.8	1.9	1.8
35SB	2.2	2.2	-	1.9	2.1	1.8	1.9
36NB	2.0	1.9	2.0	2.2	2.1	2.2	2.0
36SB	1.7	1.6	-	1.8	2.1	1.9	1.6

[a]These data were obtained by having the two-car train brake suddenly at midspan on 35NB and 36NB only.

[b]Actual measured stresses ranged from ±1.6 to ±2.3 ksi.

by using a CTA test train. Data were obtained from four- and eight-car commuter trains and two- and eight-car test trains.

Commuter Trains

The commuter trains consisted of coupled cars of the 2000, 2200, 2400, or 2600 series. Cars of different series were mixed in a single train. Strain recordings were started as the commuter train approached the point on the structure where it could be expected to have an influence on any of the strain gauges in that region.

Test Trains

Data acquisition involving the test trains was done at night by using 2600 series cars. For the dynamic tests, the motorman was instructed to maintain a constant speed of 25 mph. Data recording was initiated just before the front axle of the train reached the point where it was anticipated to have influence on the strain gauges being monitored. For the static tests, location marks were painted at 10-ft intervals on the rails. For each test, the front wheels of the test train were positioned over a location mark, data were recorded, and the train was advanced 10 ft to the next station. In this way a stress influence line was generated for each gauge. This influence line was compared with those of the dynamic runs to indicate moving train position, speed, and impact factors.

A special dynamic test was also conducted near bent 35 by using a two-car train on the northbound tracks. The train was brought up to speed and then stopped quickly at critical locations by using the emergency brakes. It was expected that this maneuver would result in additional impact loading information for the structure.

Analysis of Data

Type A Gauges Adjacent to Gusset Plate

The stresses measured adjacent to gusset plates agree reasonably well with the theoretical analyses, if a lesser axle load is used in calculations. The measured stress ranges are given in Table 2. Stresses ranged from 1.0 to about 2.5 ksi, with most of the values within 1.5 to 2.0 ksi. The agreement between gauges located adjacent to the same gusset plate was quite satisfactory. The following four observations are based on type A strain-gauge readings.

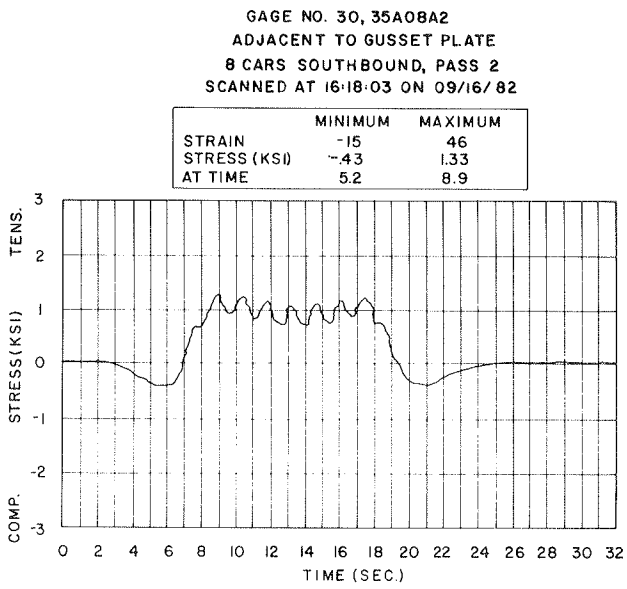

FIGURE 11 Dynamic strain response during the passage of an eight-car train.

1. In all the measured strain responses it was observed that a single train, regardless of length, induces a single large cycle of stress. A typical plot of dynamic strain response during the passage of an eight-car train is shown in Figure 11. In many cases the groupings of four axles at the ends of adjacent cars caused individual cycles to have magnitudes of up to one-third the maximum stress ranges measured. In the most extreme cases the magnitudes of the individual cycles were found to be less than about 400 psi, which is not considered to be significant.

2. Dynamic stresses are a maximum of 10 percent greater than static stresses in simply supported spans, as shown in Figures 12 and 13. In continuous spans the dynamic results are generally equal to the static results (Table 2). These effects are difficult to quantify because the differences are small.

3. As expected, the outside stringer on horizontal curves carries greater loads than the inside stringer. Figure 14 shows comparisons in stress range for geometrically similar gauge locations in adjacent stringers in three different spans. Note that there appears to be a somewhat more equal distribution of load in spans 36NB and 36SB, which are simple spans of only two stringers. The relationship

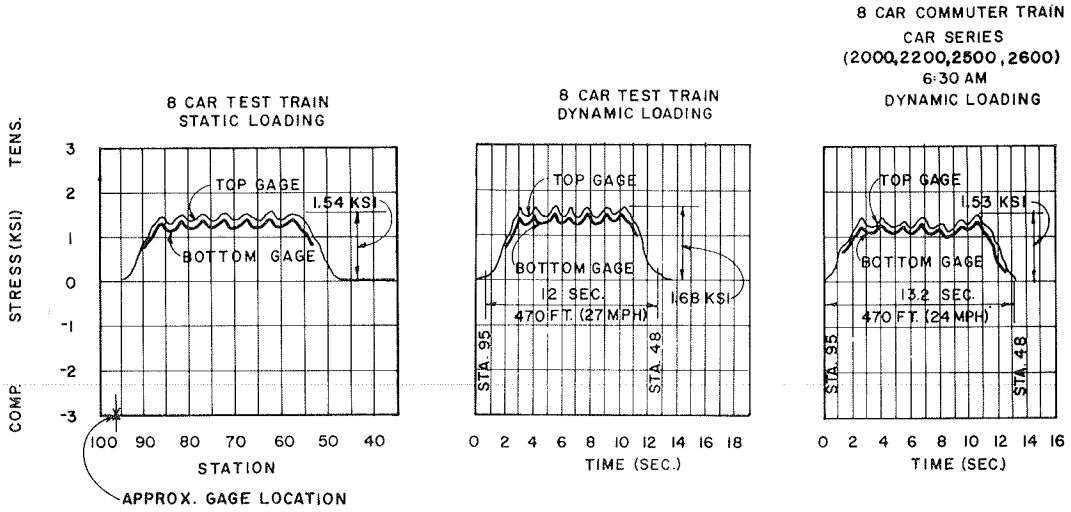

FIGURE 12 Comparison of upper and lower type A gauges in span 22 under different loading conditions.

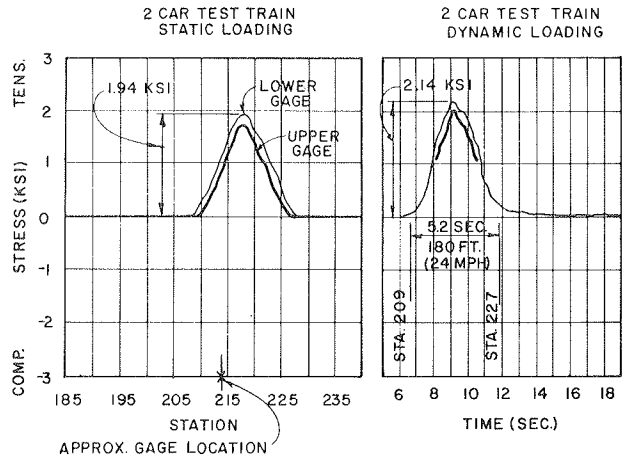

FIGURE 13 Comparison of upper and lower type A gauges in span 36 under different loading conditions.

between the radius of curvature of the stringers and the lateral distribution of loads could not be established with the amount of instrumentation used.

4. Overall, the measured stress ranges adjacent to gusset plates were less than the stress ranges predicted by the analytical studies. The average of measured stress ranges from eight-car commuter trains is 1.7 ksi. The computed value is 2.3 ksi based on 19.5 kips per axle, and 2.1 ksi for 17.5 kips per axle. The maximum measured stress range at any gauge was 2.4 ksi compared with the theoretical values of 4.0 ksi for 19.5 kips per axle or 3.5 ksi for 17.5 kips per axle. Thus measured stress ranges average 60 and 70 percent of the calculated values based on expected and design train loads of 17.5 and 19.5 kips per axle, respectively.

One of the reasons for the difference between theoretical and measured stress levels is shown in Figure 15, which compares stresses from northbound and southbound trains. These gauges are on the exterior stringer under the southbound track in spans 35 and 21. Note that the stresses from northbound trains are 18 and 39 percent of the values from southbound trains, which show the substantial lateral distribution of loads by the concrete deck and steel diaphragms. Smaller lateral stiffnesses for span 35 relative to span 21 are also indicated. Span 35 has a limited lateral bracing system between the northbound and southbound sides of the structure.

Type B Gauges on Lateral Bracing

Readings on type B gauges generally were relatively

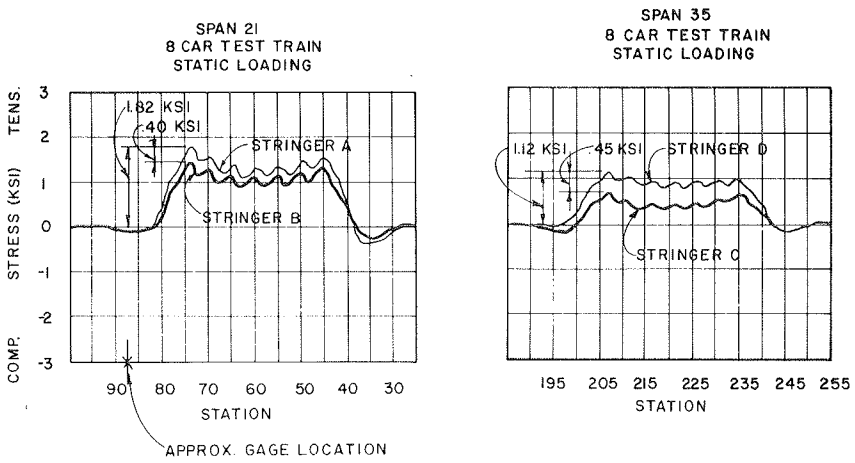

FIGURE 14 Comparison of stresses measured in type A gauges for adjacent stringers.

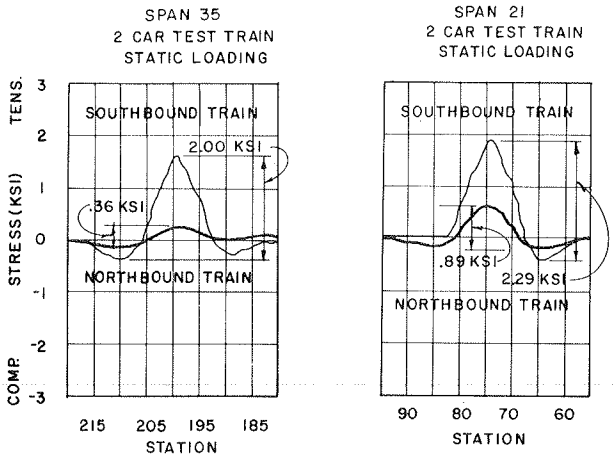

FIGURE 15 Comparison of influence of northbound and southbound trains showing lateral load distribution.

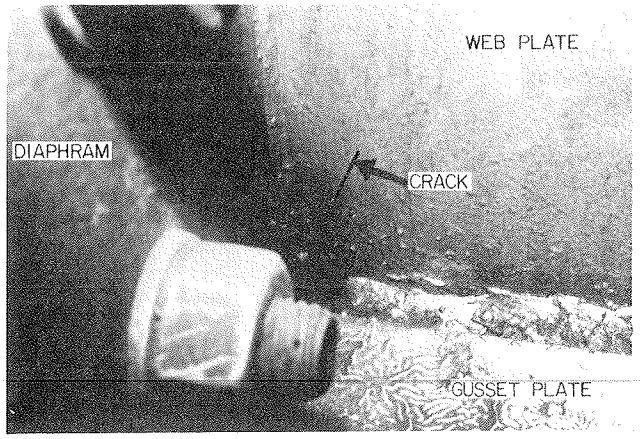

FIGURE 16 Upper segment of 4-in.-long crack found near midspan of span 16.

small, which indicated that axial forces in the bracing were low. This is to be expected, because torsional moments that would generate axial forces in the lateral bracing are generally smaller at midspan than near supports. Maximum force levels of 7 to 10 kips were indicated.

Type C Gauges on Top and Bottom Flange of Stringers

Type C gauges were placed near type A gauges in most spans to yield additional information about the distribution of stress in the stringers. It was found that the bottom flange gauges gave lower strains than type A gauges, which indicates that the gusset plates produced some stress-magnification effects. These gauges indicated strains about 15 percent greater than those measured in type C gauges.

The type C gauges also demonstrated the composite behavior assumed for the analytical model. The position of the neutral axis determined from measured strains agreed within 8 percent of the theoretical position.

Type D Gauges: Cross-Sectional Gauges in Bents and Piers

Strains were measured on the cross sections of one bent box support and two pier box supports. The measurements indicated that the neutral axis was located at approximately the mid-depth of the box section. Maximum dynamic tensile stress ranges are about 1.2, 1.0, and 0.8 ksi at bents 35 and 34 and pier 17, respectively. The dynamic stresses are roughly 20 percent higher than static values, which indicates that impact factors for box bents and piers may be somewhat higher than those measured in the stringers.

Type E Gauges on Bent 35 Web Plate Adjacent to Flange Tips of Stringers

The stresses measured in type E gauges compared well with the stresses measured on the bottom flange of bent 35. The overall indicated stress range is about 0.9 ksi under dynamic loading. Magnification of web plate strains caused by out-of-plane bending was not indicated.

Inspections of Gusset-Plate Welds

Close inspection of gusset plate to stringer web welds was made in the seven instrumented spans. The inspections concentrated on the toes of welds near the cutouts and around the ends of the gusset plates, where fatigue cracks are most likely to initiate.

The inspections were conducted by first thoroughly cleaning the area and examining it with a bright light and a magnifying glass. If any indication of a crack or discontinuity was observed, the weld toe was subjected to additional cleaning and magnetic particle inspection. If the observed discontinuity was located at either end of the gusset plate, the weld toe was lightly ground and the magnetic particle inspection was repeated. This procedure was used to verify and aid in the removal of a small defect. If the crack was located adjacent to the gusset-plate cutout (i.e., adjacent to the vertical stiffener), it was not ground out because the structural configuration at these locations prevented access to the crack origin. Nevertheless, any slight extension of a crack out of the cutout area was detected by using the inspection procedures. Altogether, more than 400 gusset plates were inspected, which represented approximately 23 percent of the total number in the structure. Typically, each gusset represented four separate inspection locations.

During the field examination one major crack and a total of 42 small cracks or cracklike indications were found. The terminology major crack is used because of its significant length (4 in.) and because it penetrated the full thickness of the stringer web. No other observed crack had these characteristics. The major crack was located adjacent to the vertical stiffener near the midspan of span 16 (see Figure 16). For comparison purposes, the crack found in span 15 is shown in Figure 7.

Approximately 20 small cracks or cracklike indications were subjected to grinding. The term cracklike indication is used to define a discontinuity that resembles a crack in a region where crack growth would be expected. All of these indications were eliminated by light grinding.

Removal and Evaluation of Samples

Two steel samples that contained cracks were removed from the webs of stringers at gusset locations in spans 15 and 16 for examination. The examination was performed by John W. Fisher at Lehigh University. It was found that the crack surface of the sample from span 15 was too corroded to yield useful information about the cause of fracture. The crack

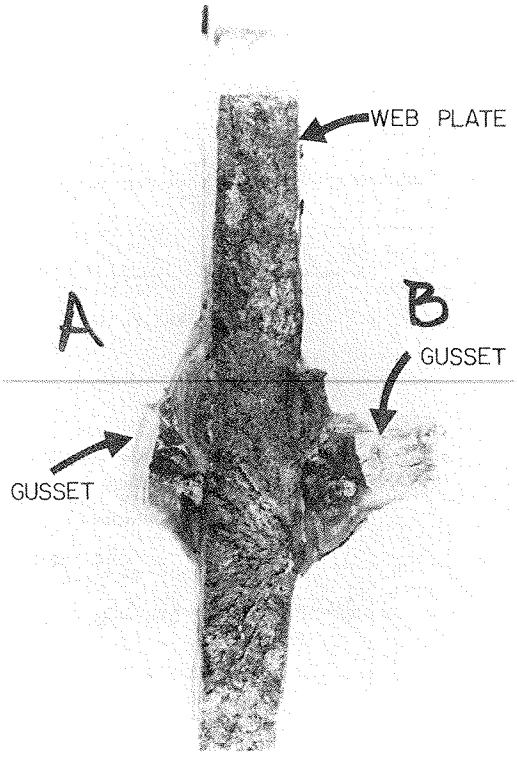

FIGURE 17 Exposed crack surface of specimen from span 16.

surface of the sample from span 16 was found to exhibit fatigue crack growth in the stringer web near the bottom surface of the gusset plate. The web plate fracture surface is shown in Figure 17. The fatigue crack was roughly elliptical in shape, its dimensions were about 0.125 in. deep by 0.375 in. long, and it exhibited fatigue crack growth striations. The striation spacing or crack growth rate was observed to vary between 1.4×10^{-6} and 5×10^{-6} in. per cycle. Figure 18 is a transmission electron microscope photograph that shows the striations. It is estimated, based on these data, that the crack after initiation can propagate to critical size after only 6 months of service.

This evaluation included a fracture mechanics analysis to predict fatigue crack growth, brittle fracture, and crack arrest. The analysis was conducted based on recommendations by Platten et al. (3). Measured stress ranges, however, were considered to be too small to have caused the cracking. Thus it is postulated that out-of-plane bending in the stringer web is occurring, which generates a stress level of 8 to 12 ksi. Unfortunately, the out-of-plane bending of the web was not shown by the strain measurements.

EVALUATION AND DISCUSSION

During this study weld details in the superstructure were carefully reviewed and classified in categories according to current AASHTO and American Railway Engineering Association (AREA) specifications (2). It was determined that the most severe condition currently in the structure is the weld junction of the lateral gusset plate to the stringer web plate. Altogether, about 1,800 lateral gusset plates are used in the 40-span stringer system.

Under current AREA specifications, the structural elements of the Dan Ryan elevated structure would be designed for varying members of constant stress

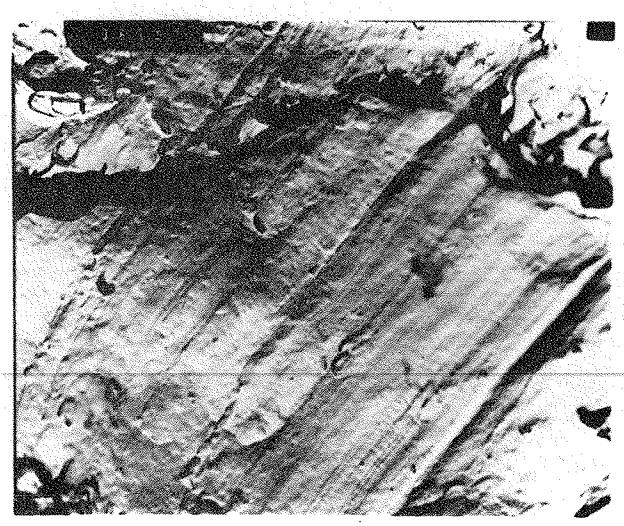

FIGURE 18 Transmission electron microscope photomicrograph: side B at 17,000X showing striation lines.

cycles caused by rail car loading according to member classification. However, the results of the test program indicate that the main consideration for all of the critical conditions is the stress range under high cyclic loading. The allowable range of stress for the various classifications of details in the structure, as defined in Table 1.3.13B of Article 1.3.13 of the AREA specifications, are given in the following table:

Stress Category	Allowable Range of Stress (S_{Rfat}) for More Than 2,000,000 Cycles (ksi)
A	24
B	16
C	12
D	7
E	5

These values are the most stringent requirements for design under AREA specifications. For a category E type detail, an allowable stress range of 5 ksi has been established.

Based on the analytical studies, a maximum stress range of 1.7 to 4 ksi was anticipated at the level of the lateral gusset-plate connection. However, the actual measured range of stress was found to vary between 1 and 2.5 ksi. The measured stresses are lower than the calculated stresses primarily because the actual train weight is lower than that used in the analysis and because of the lateral distribution of wheel loads to adjacent stringers.

The measured stress range values are less than the commonly accepted threshold for crack growth and are less than the allowable design stresses established by AREA. Therefore, typical conditions classified as category E details should exhibit satisfactory performance without fatigue crack extension. Nevertheless, the cutout between the vertical stiffener and the horizontal gusset represents a condition that is more severe than a category E detail. The small gap causes a significant magnification of stresses due apparently to out-of-plane deformation of the stringer web plate. Furthermore, the small gap makes it difficult to fabricate the detail without overlapping or intersecting welds, thus causing an unsatisfactory condition and potential built-in cracks caused by weld shrinkage and restraint. The

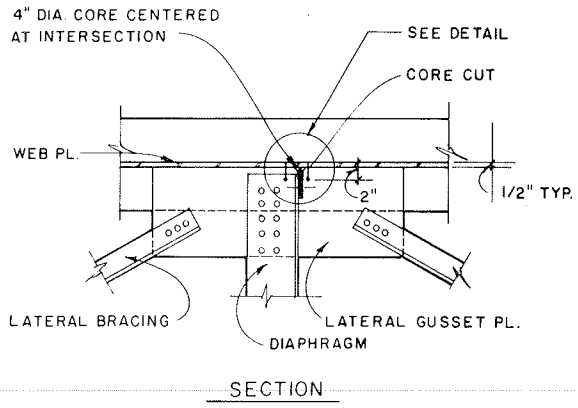

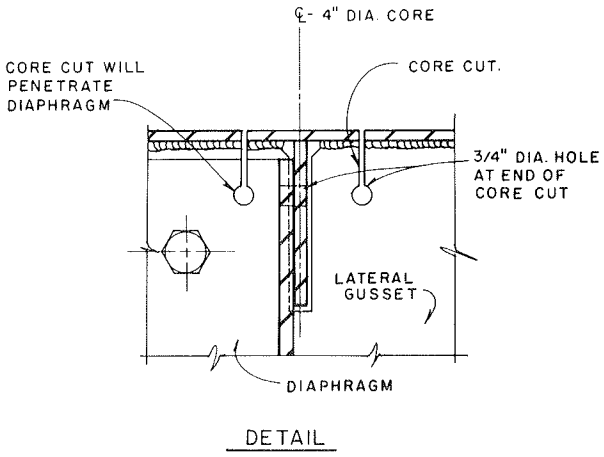

FIGURE 19 Exterior stringer retrofit by coring through web plate.

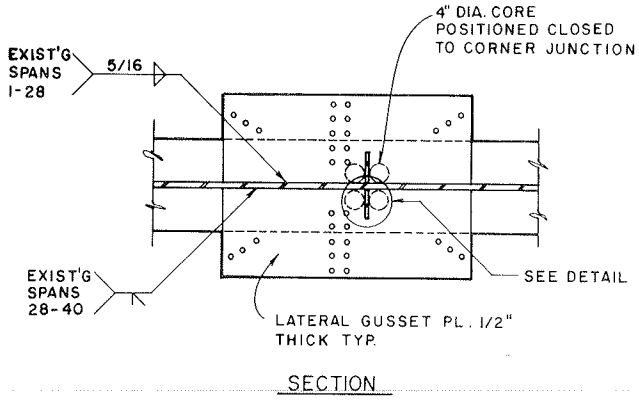

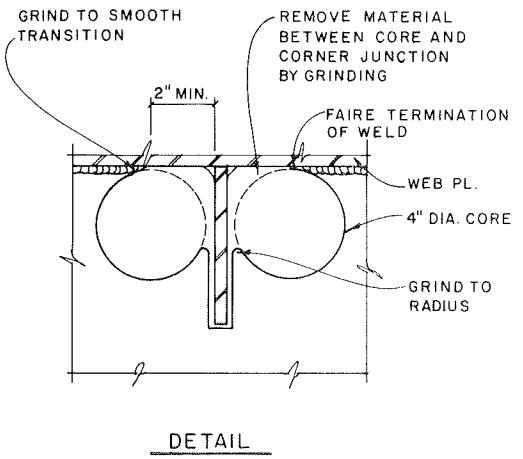

FIGURE 20 Interior stringer retrofit by coring holes through lateral gusset plate.

out-of-plane deformation of the web appears to be partly due to bending of the gusset plate by diaphragm loads and by axial loads in lateral bracing. However, the level of stress required to propagate a fatigue crack was not measured by the instrumentation used.

To date, one crack-related fracture in the stringer web adjacent to termination of a gusset-plate weld has occurred in span 15. Also, two significant cracks have been discovered. The first, in span 35, was found in early 1978 and was retrofitted. The second, in span 16, was found during the inspection of the gusset plate to stringer web welds. These major cracks all originated in the small gap at the connection between the gusset and vertical stiffener.

The crack surface in the sample from span 16 was found to have only a small fatigue portion; most of the crack was propagated by brittle fracture. Given the unsatisfactory access in the small gap, the fatigue portion is considered too small to have been discovered by visual or magnetic particle techniques.

In summary, the applicable codes indicate that fatigue should not be a problem in the structure, given the low levels of stress measured in the primary plate material. However, cracking has occurred and has been attributed to out-of-plane bending of the stringer web. The fatigue portions of cracks cannot be observed because of the confined location of the crack origin. For these reasons, a retrofitting program is essential.

RECOMMENDATIONS

The stringers require limited retrofitting to modify the lateral gusset-plate connections at the small gap. It is believed that the retrofit program may be limited to the middle third of all spans because the greatest bending stresses and differential movements between adjacent stringers occur in this region. All of the observed cracks were located within the middle third of their respective spans.

In addition, it has been recommended that the remaining 33 spans of the structure not included in this study be inspected, concentrating on the weld terminations of the lateral gusset plate to stringer web connections. The inspection of the spans in this study suggests that additional cracks may be found in the uninspected portions of the structure, and this information may alter the scope of the retrofitting program.

Two retrofit details have been developed to improve the small gap condition in the lateral gusset-plate attachment. These details are shown in Figures 19 and 20 and are described as follows.

1. Exterior stringer: This retrofit requires coring a 4-in.-diameter hole into the stringer web, as shown schematically in Figure 19. The core cutter is intended to penetrate the lateral gusset and transverse stiffener by 1.5 in. The purpose of this retrofitting procedure is to shield the fatigue-sensitive detail from stress and increase the gap width. It is intended to be used on exterior or fascia stringers.

2. Interior stringer: This procedure requires coring 4-in.-diameter holes vertically through the lateral gusset plate on both sides of the transverse stiffener. The edge of the hole along the web plate is milled or ground to achieve the profile indicated in Figure 20. The purpose of this retrofit is to increase the gap width between the gusset plate and stiffener. This modification will reduce the stress gradient in the gap region, thereby improving the fatigue life of the detail and providing a condition that will be easier to inspect.

In conjunction with the limited retrofitting program, both routine and in-depth inspections at periodic intervals should be continued. It is recommended that routine inspections be carried out on a 2-year interval, while a 10-year interval is appropriate for the in-depth inspection.

It has been concluded that the small gap condition in the lateral gusset plate has the potential for fatigue cracking and fracture. Assuming that the recommended retrofitting is carried out and a 10-year in-depth inspection program is followed, satisfactory performance of this structure should be assured.

ACKNOWLEDGMENT

This investigative study was carried out by Wiss, Janney, Elstner Associates, Inc., for the CTA. The support provided by Thomas Wolgemuth, Pat McCarthy, and Dennis Penepacker of the CTA was especially appreciated.

REFERENCES

1. The Technical Committee. Final Report on Causes of Fractures in Bent Nos. 24, 25, and 26, Dan Ryan Rapid Transit. Department of Public Works, Chicago, 1979.
2. J.W. Fisher. Bridge Fatigue Guide--Design and Details. American Institute of Steel Construction, Chicago, 1977.
3. D.A. Platten, K.H. Frank, and J.A. Yura. Analytical Study of the Fatigue Behavior of a Longitudinal Transverse Stiffener Intersection. Res. Report 247-1. Center for Transportation Research, University of Texas, Austin, Aug. 1981.

Publication of this paper sponsored by Committee on Dynamics and Field Testing of Bridges.

Post-Construction Evaluation of the Fremont Bridge

MICHAEL J. KOOB, JOHN M. HANSON, and JOHN W. FISHER

ABSTRACT

The Fremont Bridge is a three-span, stiffened-steel tied arch that is 2,159 ft long. During construction a major brittle fracture occurred in one of the box-shaped tie girders near the end of the bridge at the beginning of the arch rib. Since completion in 1973, small cracks and other discontinuities were found in welds in the vicinity of the junction of the tie girders and arch ribs. Cracks were also found in welds that connect wide flange stiffeners to the side plates of the tie girders. A comprehensive post-construction evaluation of the bridge was made to assess the long-range integrity of main load-carrying, nonredundant tensile members and components of the structure. The study included a review of drawings and records of construction, visual inspection of the tie girders, nondestructive examination of welds, field testing, an analytical review, and examination and testing of cores. The information collected during the study, particularly the testing and examination of core samples, is reviewed. Also, the evaluation of the resistance of the bridge to fatigue and fracture is summarized. As part of this study, a surveillance plan was developed that is intended to reveal crack growth in time to take corrective action.

The Fremont Bridge is a three-span, stiffened-steel tied arch that is 2,159 ft long (Figure 1). It was designed in the late 1960s (1) to meet the requirements of the ninth edition (1965) of the AASHO Standard Specifications for Highway Bridges (2). This was before the adoption of new fatigue provisions that appeared in the 1974 AASHTO Interim Specifications (3). Construction of the bridge was completed in 1973.

Under the 1978 AASHTO fracture control plan (4), the tie girders of the Fremont Bridge are classified as main load-carrying, nonredundant tensile members. There are numerous conditions in the tie girders that can be classified as category E or E', according to current AASHTO specifications.

During construction a major brittle fracture occurred in one of the tie girders near the end of the bridge at the beginning of the arch rib. As a result of this fracture, a major modification was made in the structure at this location.

Since completion of the bridge, small cracks and other defects were found in welds in the vicinity of the junction of the tie girders and arch ribs. Cracks were also found in welds that connect wide flange stiffeners to the web plates of the girders.

A comprehensive post-construction evaluation of the Fremont Bridge was made to assess the long-range integrity of main load-carrying, nonredundant tensile members and components of the structure. The study included a review of drawings and records of construction, visual inspection of the tie girders, nondestructive examination of welds, field testing,